HUNGARIAN JOURNAL
OF INDUSTRIAL CHEMISTRY
VESZPRÉM
Vol. 17. pp. 383-396 (1989)

ANALYSIS OF NONISOTHERMAL NONADIABATIC TUBULAR REACTORS IN THE PRESENCE OF EXTERNAL DISTURBANCES

Y. S. SRINIVAS, V. K. JAYARAMAN and B. D. KULKARNI

(Division of Chemical Engineering National Chemical Laboratory Pune-411 008 INDIA)
Received: January 18, 1989

A nonisothermal nonadiabatic tubular reactor was analyzed in the presence of external disturbances. The study, while not revealing any noise induced transitions, clearly shows the preference of evolving states in the presence of noise.

Introduction

Multiple steady states are known to exist in nonisothermal nonadiabatic systems for a certain range of parameter values [1, 2]. It has been elucidated that in a certain region of Damkohler numbers five steady states classified as kinetic, diffusion and intermediate regimes are possible. The results of the effects of the external fluctuations on the system behaviour are reported here.

Attention is restricted to a simple reaction $A \rightarrow B$ accompanied by the evolution of heat. If a chemical reaction is accompained by heat effects, then the transient behaviour of the system is described by a set of parabolic partial differential equations. The assumptions underlying the developments are [3]: no radial velocity and concentration gradients in the reactor, the temperature gradient may be described by the use of a proper value of the effective radial conductivity, absence of temperature and concentration gradients within and outside of a catalyst particle, the properties of a reaction mixture may be characterized by average values, and the mechanism of axial mixing can be described by means of a single parameter in the Fick's or Fourier's law respectively. The heat and mass balances can then be written in the dimensionless form [3]:

$$\frac{\partial y}{\partial t} = \frac{1}{Pe_y}\frac{\partial^2 y}{\partial z^2} - \frac{\partial y}{\partial z} + \mathrm{Da}(1-y)\exp\left(\frac{\theta}{1+\theta/\gamma}\right) \tag{1}$$

$$\frac{\partial \theta}{\partial t} = \frac{1}{Pe_\theta}\frac{\partial^2 \theta}{\partial z^2} - \frac{\partial \theta}{\partial z} + \mathrm{B\,Da}(1-y)\exp\left(\frac{\theta}{1+\theta/\gamma}\right) - \beta(\theta-\theta_c) \tag{2}$$

where y is dimensionless conversion, $y \in [0, 1]$; θ is the dimensionless temperature, γ is dimensionless activation energy, Pe_y is the Peclet number for axial mass transport, Pe_θ is the Peclet number for axial heat transport, B is the dimensionless parameter of heat evolution, θ_c is the dimensionless cooling temperature and β is the heat transfer parameter. All parameters are positive, but θ_c can also be negative.

The corresponding boundary conditions chosen here are:

$$z=0: \quad Pe_y y = \frac{\partial y}{\partial z}; \quad Pe_\theta \theta = \frac{\partial \theta}{\partial z} \tag{3}$$

$$z=1: \quad \frac{\partial y}{\partial z} = \frac{\partial \theta}{\partial z} = 0 \tag{4}$$

The variables and the parameters used in the dimensionless formulation are:

$$Pe_\theta = \frac{\varrho v c_p l}{k_e} \quad Pe_y = \frac{vl}{D_e} \quad B = \frac{(-\Delta H)C_0}{\varrho c_p T_0} \frac{E}{RT_0}$$

$$\gamma = E/RT_0 \quad \beta = \frac{4H}{\varrho v c_p} \frac{l}{D_e} \quad \theta = \frac{E}{RT_0^2}(T-T_0)$$

$$\theta_c = \frac{E}{RT_0^2}(T_c - T_0) \quad z = \frac{x}{l} \quad t = \frac{t'v}{l}$$

The external noise can be incorporated into the above model by the following Ornstein-Uhlenbeck equation:

$$\frac{d\xi}{dt} = -\frac{1}{\tau}\xi + \frac{\sigma}{\sqrt{\tau}}\left(\frac{dW}{dt}\right) \tag{5}$$

where ξ is the noise term, σ is the strength of the noise and τ the correlation time. The distribution chosen here for the random generation is of the Gaussian type.

Damkohler number, D_a, is taken as the parameter to be fluctuating and the noise term ξ is incorporated into this parameter. The resulting stochastic equations of the axial mass and heat transports by the incorporation of noise are given by:

$$\frac{\partial y}{\partial r} = \frac{1}{Pe_y}\frac{\partial^2 y}{\partial z^2} - \frac{\partial y}{\partial z} + (\mathrm{Da} + \xi/\varepsilon)(1-y)\exp\left(\frac{\theta}{1+\theta/\gamma}\right) \tag{6}$$

$$\frac{\partial \theta}{\partial t} = \frac{1}{Pe_\theta}\frac{\partial^2 \theta}{\partial z^2} - \frac{\partial \theta}{\partial z} + \mathrm{B}(\mathrm{Da} + \xi/\varepsilon)(1-y)\exp\left(\frac{\theta}{1+\theta/\gamma}\right) - \beta(\theta - \theta_c) \tag{7}$$

Numerical Methods of Solution of Transport Equations

Equations (5), (6) and (7) have to be simultaneously solved along with the boundary conditions given by Equations (3) and (4). To generate the solution or dependence diagram a mapping technique [4] was used and solved numerically. The calculation of steady state profiles from Equations (1–4) represents a

difficult problem. For this purpose, a shooting procedure [5] was used with a backward integration from $z=1$ to $z=0$. The partial differential equations [Equations (6) and (7)], were solved by the method of finite differences [6] with the noise term ξ incorporated. This was achieved by a random noise generator of the Gaussian distribution and Equation (5), solving them by fourth order Runge-Kutta method.

Results and Discussion

Figure 1 gives the dependence of exit temperature and exit concentration on the value of Damkohler number (Da). This figure shows a loop like dependence of $\theta(l)$ on $f(Da)$. For a certain small range of Da as shown in *Figure 1*, the system admits the existence of the five steady states. The different steady states are marked as 1, 2, 3, 4 and 5 for the value of $Da=0.07$. For the steady state 1, the exit temperature and conversion is low. This steady state is referred to as the "kinetic profile". The steady state 5 corresponds to the "diffusion profile"

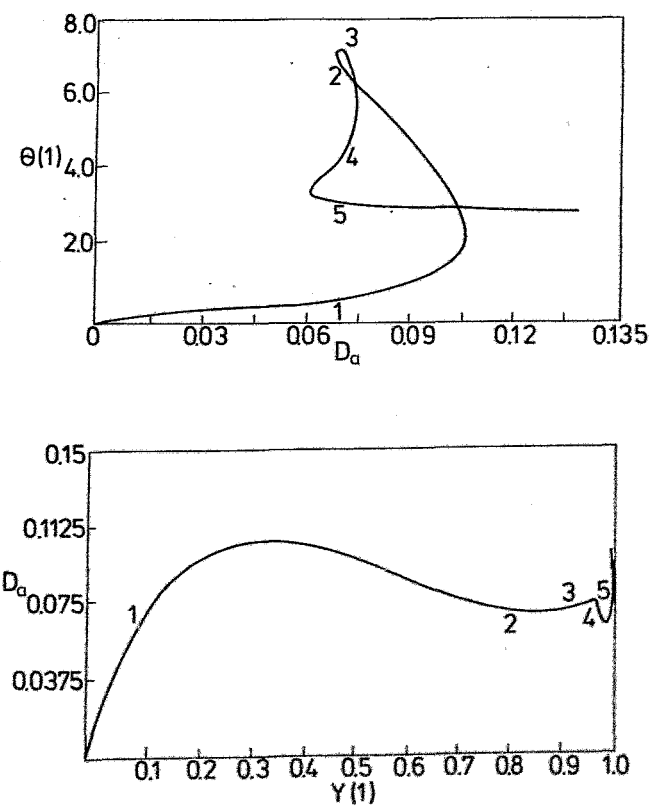

Figure 1.

observed for adiabatic reactors. Here the axial mass and heat dispersion are the rate determining steps. The steady state 3 occurs over a narrow range of *Da* values and exists only for nonadiabatic systems and is termed as the "intermediate regime". It was reported earlier that for high values of both B and β the "intermediate regime" vanishes [1].

Figure 1 reveals that the hysteresis loop is of the type

kinetic regime → diffusion regime → kinetic regime

i.e. an increase of the value of *Da* gives rise to a jump towards the "diffusion regime". The extinction process is a jump from the diffusion branch to the kinetic branch.

The deterministic analysis reveals that the steady state 1, representing the "kinetic profile", and steady state 5, representing the "diffusion profile" are stable. The stochastic analysis was performed on both the stable and unstable profiles, and the corresponding results show a marked change in the stability properties from that of the deterministic analysis, which was shown in the subsequent figures. These results are classified under the "effect of τ (correlation time)" and the "effect of σ (strength of noise)".

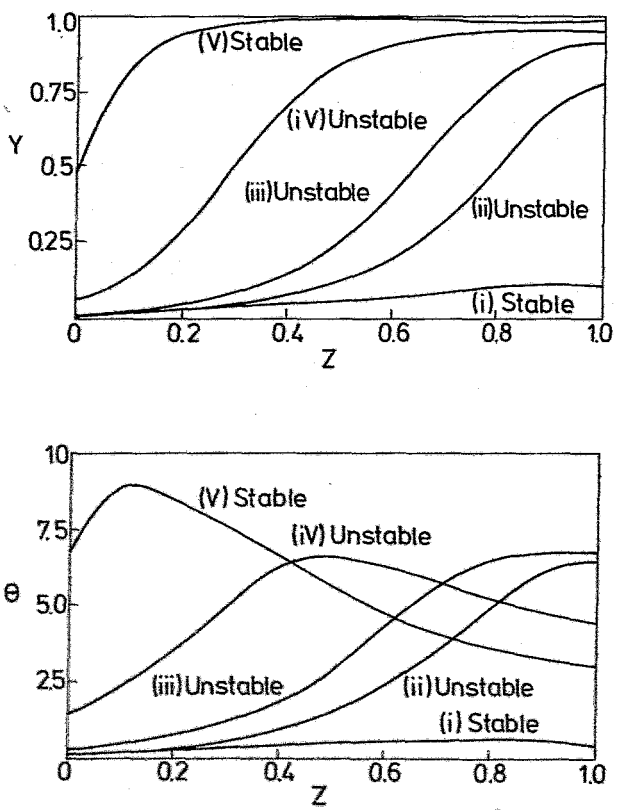

Figure 2.

Figure 2 reveals the steady state profiles (i, ii, iii, iv and v) of the five steady state region solutions [1, 2, 3, 4 and 5 respectively of *Figure 1*] of both the mass and temperature variables. The profiles indicate how the steady states 1, 2, 3, 4 and 5 (see *Figure 3.1*) look in the space dimension for the dimensionless concentration and dimensionless temperature. The Newton-Fox shoot method [5] was employed to evolve these spatial profiles. The point '1' on *Figure 1* indicates the exit values (i.e. at $z = 1$) of the dimensionless concentration (y) and dimensionless temperature (θ). For these exit values, a guess is made for the corresponding inlet values of y and θ. A backward shooting technique was used, where a guess is made at one boundary ($z = 0$), and the integration was iterated until the boundary condition at the other end ($z = 1$) was matched. These profiles evolved by the shoot algorithm are given in this Figure, and represent the steady state values of y and θ in the space dimension; the same were taken as initial profiles for the subsequent deterministic and stochastic analyses.

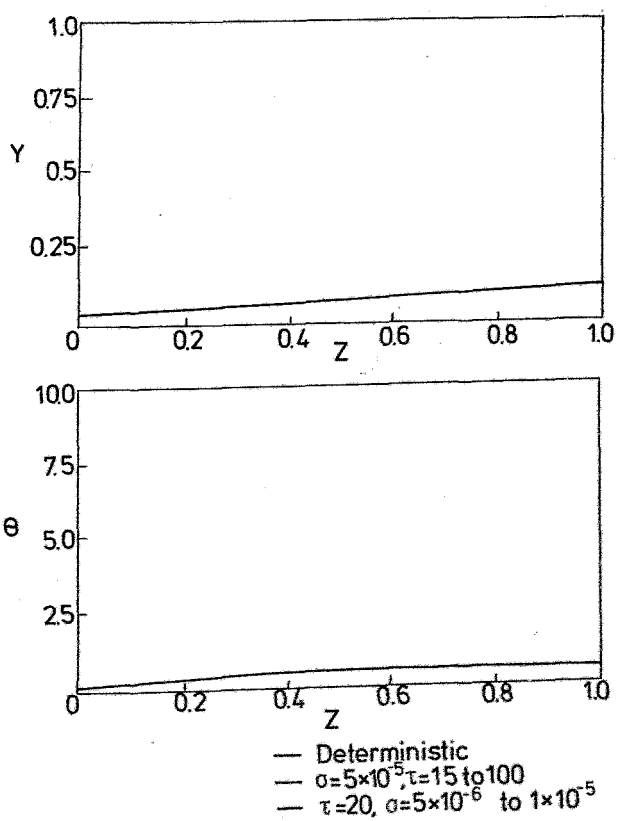

Figure 3.

Figures 3 and *4* reveal the results of deterministic and stochastic analyses performed on the "kinetic profile (i)" of *Figure 2*. *Figure 3* depicts the spatial profiles of the dimensionless concentration and dimensionless temperature for different values of the noise intensity and the noise correlation time. The parabolic partial differential equation representing axial mass and heat dispersion was simultaneously solved for both the deterministic and stochastic evolution. The concentration profile (i) (see *Figure 2*), was taken as the initial condition for the finite difference approach. The single profile, marked as deterministic (in the absence of noise) in *Figure 3*, is the solution profile that eventually reached a steady state, after a certain magnitude of time ($t = 15$). In other words, it means that the initial profile (i) we started with, evolves in a time dimension and stabilises as shown in *Figure 3*. The same initial profile (i) was subjected to external fluctuations for varying noise strengths ($\sigma = 5 \times 10^{-6}$ to

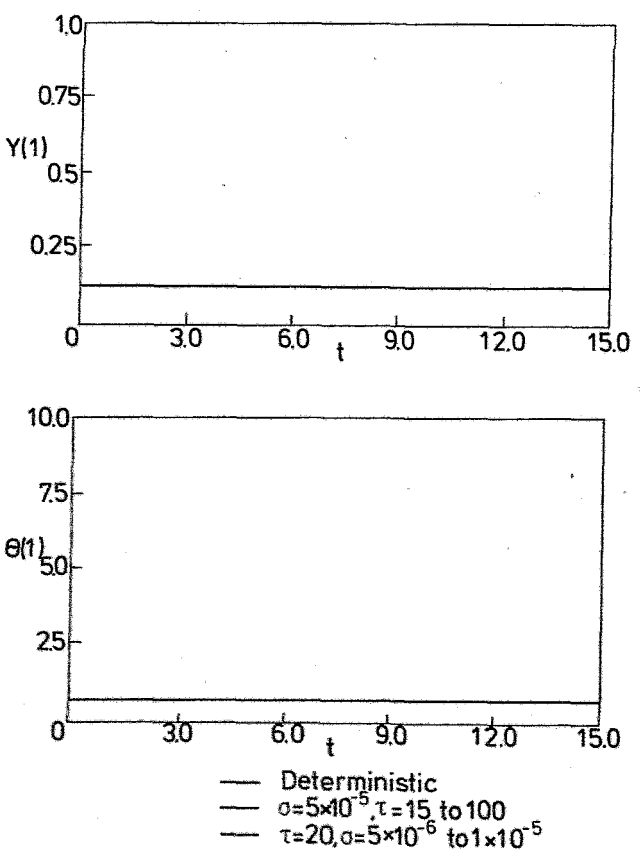

Figure 4.

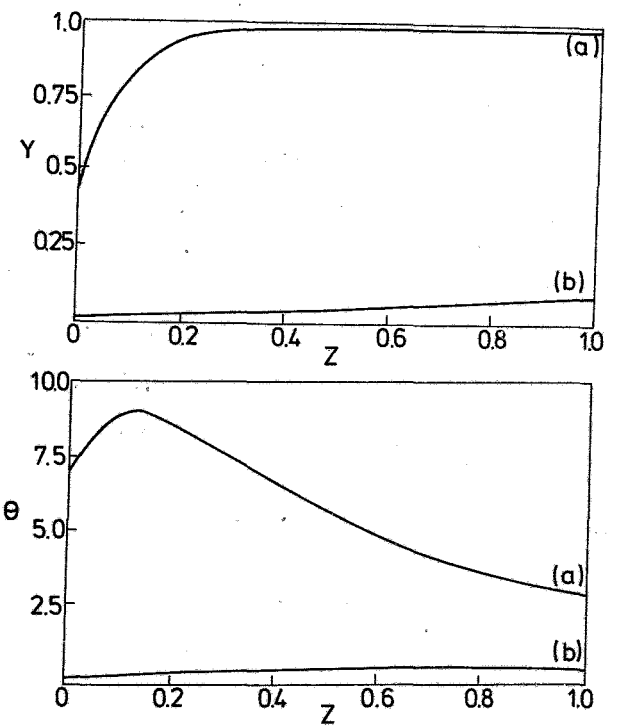

Figure 5.

1×10^{-5}) at a fixed noise correlation time ($\tau = 20$) and varying noise correlation times ($\tau = 15$ to 100) at a fixed noise intensity ($\sigma = 5 \times 10^{-5}$). In this particular case, the effect of these external fluctuations had no effect whatsoever, and hence the stochastically evolved profile conforms to that of the deterministically evolved. Hence one can conclude that the system operating in the "kinetic regime" is a remarkably stable state.

Over the subsequent stochastic analysis of the other steady states 2, 3, 4 and 5 (see Figure 1), it was observed that the magnitude of the macroscopic time variable ($t = 15$), is sufficient for any of these states to reach a steady value. In the Figures to follow, the spatial profiles of y and θ are those profiles at $t = 15$. The temporal profiles, depicted in the Figures to follow, show how these variables (y and θ) evolve in the time dimension to reach a steady state. These are drawn with the variable values at $z = 1$ i.e. $y(1)$ and $\theta(1)$ and hence depict the exit concentrations and temperatures at various times.

Figures 5 and *6* give the results of both deterministic and stochastic analyses of initial profile (ii) (see *Figure 2*). The deterministic analysis reveals that the system operating in the steady state region corresponding to point '2' of *Figure 1* stabilizes in the "diffusion regime", i.e. profile (v) (see *Figure 2*). The corresponding stochastic profile showing the effect of τ is also depicted in the Figures. It is observed from the above plots that a slight change of τ, above $\tau = 15$, brings the system to the "kinetic regime", i.e. profile (i), which otherwise (deterministically) would have led to a "diffusion regime" (i.e. profile (v) of *Figure 2*). The system which originally was diffusion controlled, with the fluctuation of the dependence parameter *Da*, would now be kinetically controlled. The temporal evolution of the dimensionless concentration y and dimensionless temperature θ is given in *Figure 6*. The effect of σ was realized and it was observed that for

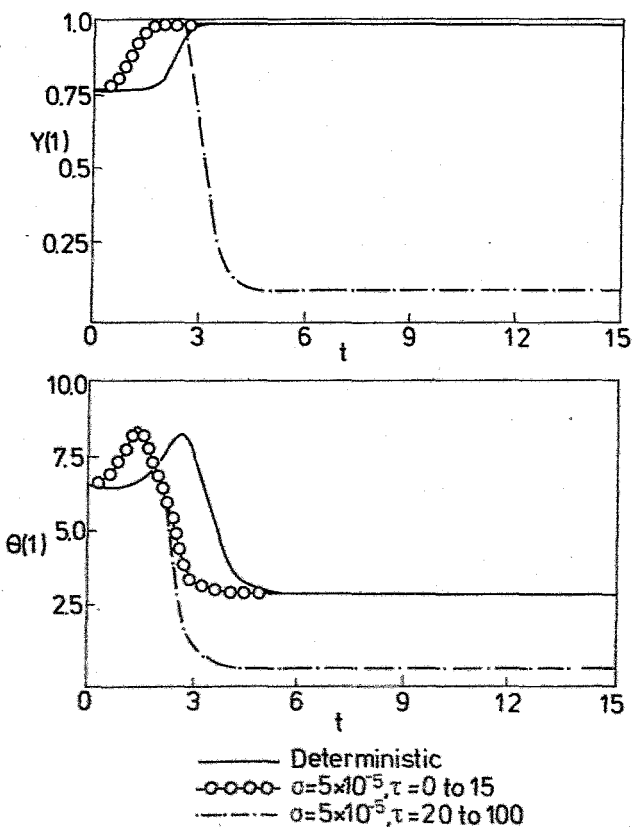

Figure 6.

a particular value of $\tau = 20$, even a marked increase in σ always brings the system to the kinetic profile (i). This is marked as profile (b) in *Figure 5*.

One can notice that the "intermediate regime", profile (iii) (see *Figure 2*), which stabilizes at the kinetic profile (i), reverses its trend by going to the diffusion profile (v) upon the incorporation of fluctuations *(Figures 7* and *8)*. An interesting feature one can observe is that even a slight fluctuation (of the order of 0.49% to 0.82%) would make the system shift from the "kinetic regime" to the "diffusion regime". This stability shift is only between limits of $\tau = 0.6$ and 1.7, and $\sigma = 5 \times 10^{-8}$, below and above which the noise does not have any effect *(Figure 7)*. The surprising feature that was observed is the consistency of the effect of σ. For a fixed value of $\tau = 20$ and varied values of $\sigma = 5 \times 10^{-8}$ to 1×10^{-5}, whatever the intensity of noise, there is no marked change in the temporal as well as the spatial profiles of the concentration and temperature variables.

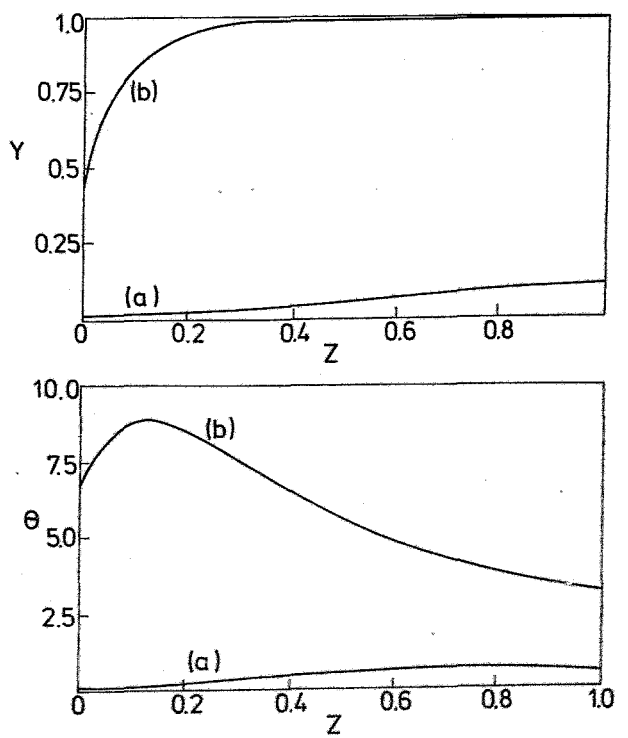

(a)- Deterministic; $\sigma = 5 \times 10^{-8}$, $\tau < 0.5$, $\tau > 1.8$
(b)- $\sigma = 5\ 10^{-8}$, $\tau = 0.6$ to 1.7

Figure 7.

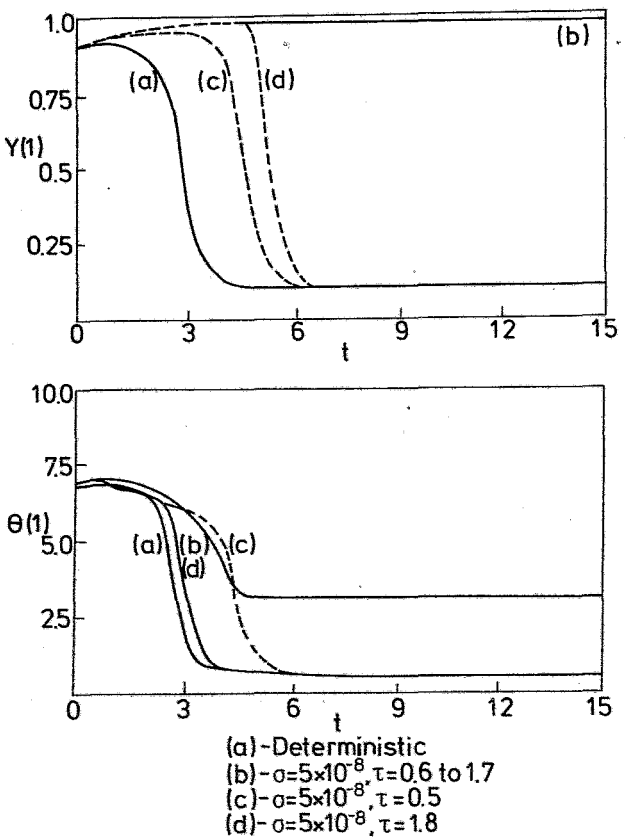

Figure 8.

The deterministic and stochastic analyses results of profile (iv) are depicted in *Figures 9* and *10*. The effect of τ and σ can be qualitatively seen to be the same as that for the "intermediate regime", i.e. profile (iii). The percentage noise used for this analysis is higher compared to the previous profile. Though the temporal evolution varies initially slightly, there is not much of a marked difference in the qualitative features from that of profile (iii) *(Figures 9* and *10)*. It is also observed that the effect of σ, for $\tau = 50$, is to bring the system to profile (v) (the "diffusion regime") for whatsoever the noise intensity may be.

The diffusion profile (v) which was stable in the deterministic analysis was found to stabilize in the kinetic regime, upon the incorporation of noise, thus revealing that the diffusion controlled solution profile would no longer exist.

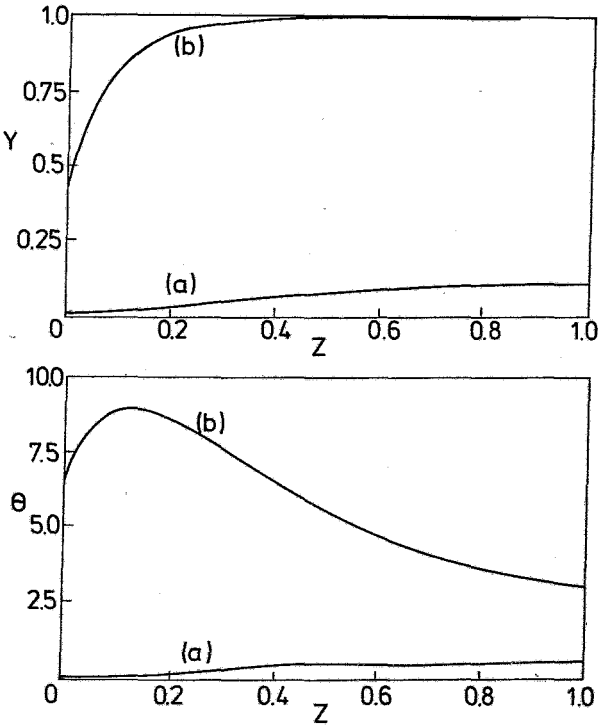

(a) - Deterministic; - $\sigma = 5\times10^{-5}, \tau = 0$ to 14

(b) - $\sigma = 5\times10^{-5}, \tau = 15$ to 94; - $\tau = 50, \sigma = 5\times10^{-8}$ to 5×10^{-6}

Figure 9.

Conclusions

The overall conclusions from the above qualitative study of the five steady state regimes is that the kinetic profile (i) is deterministically and stochastically stable. The diffusion profile (v) stabilises to the kinetic profile regime.

The system initially at an unstable steady state, which would have evolved to a steady state in a kinetic regime, now under the influence of noise, evolves to the other steady state in a diffusion regime, thus showing a total reversal.

SYMBOLS

B dimensionless adiabatic temperature
C concentration
C_0 initial concentration

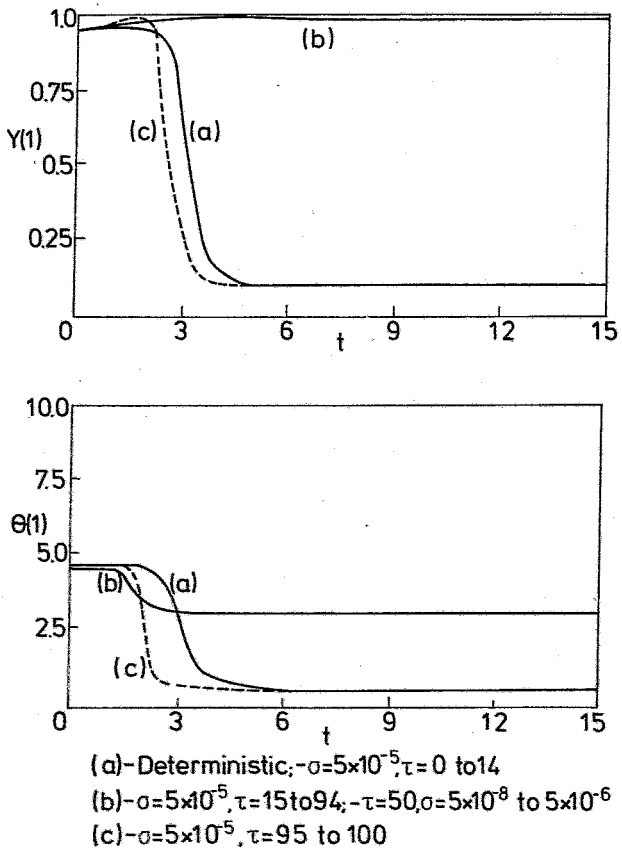

Figure 10.

c_p	specific heat at constant pressure
D_a	Damkohler number
D_e	effective conductivity in axial direction
E	activation energy
H	heat transfer coefficient
k_e	effective conductivity in axial direction
k_0	initial rate constant
l	length of reactor
Pe_y	Peclet number for axial mass transport
Pe_θ	Peclet number for axial heat transport
R	gas constant
t	dimensionless time
t'	time
T	temperature
T_0	initial temperature

v linear velocity
W Wiener process variable
x axial coordinate
y conversion
z dimensionless axial coordinate
β dimensionless heat transfer parameter
θ dimensionless temperature
θ_c dimensionless cooling temperature
γ dimensionless activation energy
ϱ density
$(-\Delta H)$ heat of reaction
τ correlation time of noise
σ intensity of the noise
ε $\frac{1}{\tau}$

LITERATURE

1. KUBICEK, M. and MAREK, M.: Chem. Eng. Sci. *1979*, 34, 593.
2. HLAVACEK, V. and HOFMANN, H.: Chem. Eng. Sci. *1970*, 25, 1517.
3. HLAVACEK, V. and HOFMANN, H.: Chem. Eng. Sci. *1970*, 25, 173.
4. HLAVACEK, V. and KUBICEK, M.: "Numerical Solution of Nonlinear Boundary Value Problems with Applications", Prentice-Hall, 1983.
5. KUBICEK, M. and MAREK, M.: "Computational Methods in Bifurcation Theory and Dissipative Structures", Springer-verlag, 1983.
6. ALKIS CONSTANTINIDES: "Applied Numerical Methods with Personal Computers", McGraw-Hill, New York (1987).